

Local thermal non-equilibrium in sediments: Implications for temperature dynamics and the use of heat as a tracer

Roshan, H.; Cuthbert, Mark; Andersen, M.S.; Acworth, R.I.

DOI:

[10.1016/j.advwatres.2014.08.002](https://doi.org/10.1016/j.advwatres.2014.08.002)

License:

Other (please specify with Rights Statement)

Document Version

Peer reviewed version

Citation for published version (Harvard):

Roshan, H, Cuthbert, M, Andersen, MS & Acworth, RI 2014, 'Local thermal non-equilibrium in sediments: Implications for temperature dynamics and the use of heat as a tracer', *Advances in Water Resources*, vol. 73, pp. 176-184. <https://doi.org/10.1016/j.advwatres.2014.08.002>

[Link to publication on Research at Birmingham portal](#)

Publisher Rights Statement:

NOTICE: this is the author's version of a work that was accepted for publication in *Advances in Water Resources*. Changes resulting from the publishing process, such as peer review, editing, corrections, structural formatting, and other quality control mechanisms may not be reflected in this document. Changes may have been made to this work since it was submitted for publication. A definitive version was subsequently published in *Advances in Water Resources* [VOL 73, November 2014] DOI: 10.1016/j.advwatres.2014.08.002

Eligibility for repository checked October 2014

General rights

Unless a licence is specified above, all rights (including copyright and moral rights) in this document are retained by the authors and/or the copyright holders. The express permission of the copyright holder must be obtained for any use of this material other than for purposes permitted by law.

- Users may freely distribute the URL that is used to identify this publication.
- Users may download and/or print one copy of the publication from the University of Birmingham research portal for the purpose of private study or non-commercial research.
- User may use extracts from the document in line with the concept of 'fair dealing' under the Copyright, Designs and Patents Act 1988 (?)
- Users may not further distribute the material nor use it for the purposes of commercial gain.

Where a licence is displayed above, please note the terms and conditions of the licence govern your use of this document.

When citing, please reference the published version.

Take down policy

While the University of Birmingham exercises care and attention in making items available there are rare occasions when an item has been uploaded in error or has been deemed to be commercially or otherwise sensitive.

If you believe that this is the case for this document, please contact UBIRA@lists.bham.ac.uk providing details and we will remove access to the work immediately and investigate.

Accepted Manuscript

Local thermal non-equilibrium in sediments: implications for temperature dynamics and the use of heat as a tracer

H. Roshan, M.O. Cuthbert, M.S. Andersen, R.I. Acworth

PII: S0309-1708(14)00155-9

DOI: <http://dx.doi.org/10.1016/j.advwatres.2014.08.002>

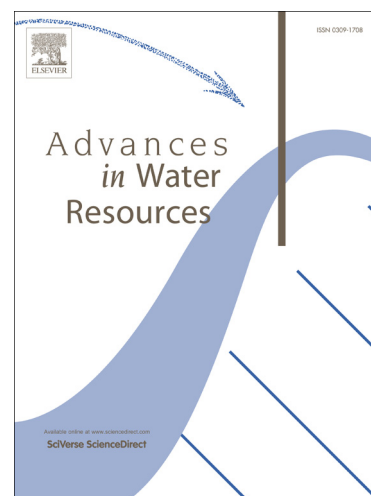
Reference: ADWR 2249

To appear in: *Advances in Water Resources*

Received Date: 28 January 2014

Revised Date: 23 June 2014

Accepted Date: 2 August 2014



Please cite this article as: Roshan, H., Cuthbert, M.O., Andersen, M.S., Acworth, R.I., Local thermal non-equilibrium in sediments: implications for temperature dynamics and the use of heat as a tracer, *Advances in Water Resources* (2014), doi: <http://dx.doi.org/10.1016/j.advwatres.2014.08.002>

This is a PDF file of an unedited manuscript that has been accepted for publication. As a service to our customers we are providing this early version of the manuscript. The manuscript will undergo copyediting, typesetting, and review of the resulting proof before it is published in its final form. Please note that during the production process errors may be discovered which could affect the content, and all legal disclaimers that apply to the journal pertain.

**Local thermal non-equilibrium in sediments: implications for temperature dynamics
and the use of heat as a tracer**

Corresponding author: H. Roshan, Connected Waters Initiative Research Centre, University
of New South Wales, 110 King St, Manly Vale, NSW 2093, Australia and National Centre
for Groundwater Research and Training, Australia
h.roshan@unsw.edu.au

M. O. Cuthbert, Connected Waters Initiative Research Centre, University of New South
Wales and Water Sciences (Hydrogeology), School of Geography, Earth and Environmental
Sciences, University of Birmingham, UK

M. S. Andersen, Connected Waters Initiative Research Centre, University of New South
Wales and National Centre for Groundwater Research and Training, Australia

R. I. Acworth, Connected Waters Initiative Research Centre, University of New South Wales
and National Centre for Groundwater Research and Training, Australia

Abstract

Understanding streambed thermal processes is of fundamental importance due to the effects of temperature dynamics on stream ecology and solute exchange processes. Local Thermal Equilibrium (LTE) between fluid and solid is usually assumed for modelling heat exchange in streambeds and for inferring pore water flow velocities from streambed temperature data. By examining well established experimental and theoretical relationships of the fluid-solid heat transfer coefficient in a numerical scheme for a range of Reynolds (Re) numbers ($0.01 > Re > 0.001$), we show here that, for a range of typical streambed conditions, LTE is not attained. Thus errors in velocity estimates obtained when inverting streambed temperature data assuming LTE can be considerable especially at relatively low flow rates. We show that for certain conditions where the LTE assumption is not valid, inferred pore water velocities of up to 1 m/d can be obtained with LTE assumption even if the actual velocities are much smaller or even zero. Ignoring the possibility of Local Thermal Non-Equilibrium (LTNE) will have consequences for the correct estimation of streambed pore water and heat fluxes at low Re values. More laboratory studies are urgently needed to supplement the sparse existing data in this area and further test the findings of this study.

Keywords: *Local thermal non-equilibrium, Heat as a tracer, Heat transfer, streambed*

1. Introduction

Understanding streambed temperature dynamics is critical to deriving deeper insights into stream ecology. Temperature is a fundamental biological variable and is a major control on biogeochemical processes which underpin vital ecosystem services [1]. Moreover, measurements of temperature variability between streams and groundwater [2] can be used to infer patterns and processes of hyporheic exchange [3] and are critical for controlling nutrient and carbon cycling in streambed systems and the potential attenuation of contaminants in the hyporheic zone [4]. Most techniques which use heat as a tracer rely on a physically based model which inverts temperature measurements to infer flow rates and sediment thermal properties [5]. The most popular methods take advantage of the solar signal which generally induces heat exchange between streams and underlying sediments [6-9]. A damping and attenuation of the diel stream temperature signal with depth is normally observed and most methods assume a 1-D flow field for interpretation, although recent studies have shown that this

may be problematic in real, non-uniform, flow fields [10, 11]. Additional uncertainties may stem from sediment heterogeneity [12], measurement error and difficulties in estimating thermal parameters [13, 14].

Despite its increasing popularity in the hydrological community, all studies to date which have used heat as a tracer for investigating groundwater-surface water interactions in streambed environments have assumed the validity of the single-temperature (i.e. using a single domain to model temperatures for the solid and fluid in combination) heat transport equation. This relies on the assumption of instantaneous local thermal equilibrium between the solid matrix materials and the pore fluids. However, we show here, by drawing on the extensive literature on this subject from other fields and proposing a new correlation, that this assumption is questionable in the context of many streambeds. As a result, considerable errors in flux estimation and conceptual understanding of streambed thermal processes may result.

2. Methods

2.1 Deriving the heat transfer coefficient at low Reynolds numbers typical of streambeds

When the assumption of LTE is suspected to break down, the temperature of solid and fluid phases have to be considered separately rather than as a single average temperature field. In this two-domain approach, it is assumed that each phase is continuous and represented by an appropriate effective total thermal conductivity and therefore effective thermal diffusivity [15, 16]. We use a *Dispersion-Particle-Based* two-equation model based on the heat transfer coefficient between the solid and the fluid phases. The equations for the solid and the fluid phases without heat sources or sinks and without an energy term for viscous-work can be expressed as [17, 18]:

$$\frac{\partial T^f}{\partial t} + \vec{v} \cdot \frac{\partial T^f}{\partial \vec{x}} = \frac{1}{\phi} \left(\frac{k_f}{(\rho c_p)_f} + f \left(\vec{\beta}, \vec{v} \right) \right) \frac{\partial^2 T^f}{\partial x^2} + \frac{h_{sf} a_{sf}}{\phi (\rho c_p)_f} (T^s - T^f) \quad (1)$$

$$\frac{\partial T^s}{\partial t} = \frac{k_s}{(1-\phi)(\rho c_p)_s} \frac{\partial^2 T^s}{\partial x^2} - \frac{h_{sf} a_{sf}}{(1-\phi)(\rho c_p)_s} (T^s - T^f) \quad (2)$$

Where, a_{sf} is the surface area of particle per unit volume of porous media, h_{sf} is the heat transfer coefficient, ϕ is the overall porosity and k is the thermal conductivity tensor, respectively where f represents the fluid phase and s represent the solid phase. Also $(\rho c_p)_f$ is

the volumetric heat capacity of fluid, $(\rho c_p)_s$ is the volumetric heat capacity of solid, T^f is the

fluid temperature, T^s is the solid temperature and t is the time. In addition $f(\vec{\beta}, \vec{v})$ is the

hydrodynamic dispersion function: $f(\vec{\beta}, \vec{v}) = \vec{\beta} \cdot \left(\frac{\rho_f c_f}{\rho c} \cdot \vec{v} \right)^2$ proposed by Rau et al. [19]

where $\vec{\beta}$ is the thermal dispersivity matrix and \vec{v} is the average pore water velocity defined as a vector. In this form of the hydrodynamic dispersion function the thermal dispersivity has the units of [T]. In Eqs. 1 and 2, the surface area of particles per unit volume of porous media can be estimated by [20]:

$$a_{sf} = \frac{6(1-\phi)}{dp} \quad (3)$$

Where, dp is defined as the average grain size of the porous media as would be obtained from a grain size distribution curve. It should be noted that this equation may not be valid for poorly sorted sediment, but is applicable to the homogeneous conditions modelled here. In order to determine the heat transfer coefficient between the fluid and solid particles, a number of experimental correlations have been proposed [21-23]. However, despite extensive effort, no theory has been developed which can satisfactorily describe the heat transfer rate over a wide range of porous media with different physical properties, such as grain size or velocity distribution [21]. At high Reynolds numbers, there is a well-accepted correlation which has been used to solve the heat transfer in porous beds for more than three decades. It is expressed as [21]:

$$Nu = 2 + 1.1 Pr^{\frac{1}{3}} Re^{0.6} \quad (4)$$

where, Nu , Pr and Re are the dimensionless Nusselt number, Prandtl number and Reynolds number defined as:

$$Nu = \frac{h_f dp}{k_f}, \quad Pr = \frac{c_{pf} \mu_f}{k_f}, \quad Re = \frac{\rho_f v dp}{\mu_f} \quad (5)$$

where, μ_f , c_{pf} and ρ_f are the fluid viscosity, fluid heat capacity and fluid density. Increase in Re enhances heat and momentum transfer between fluid particles which increases the friction

force on the grain surface and therefore the heat transfer rate. The average grain thermal Peclet number (Pe_{avg}) describes the ratio of the advective to conductive heat transport and defined as:

$$Pe_{avg} = \frac{\rho_f c_{pf} v dp}{k_e} \quad (6)$$

where, k_e is the average heat conductivity of the porous medium defined as $k_e = k_s^{(1-\phi)} \cdot k_f^{(\phi)}$. The proposed correlation (equation 4) explains the experimental data obtained by many authors [24, 25] for $Re > 1$. However, such high Re are not expected in streambeds unless the grainsize and thus hydraulic conductivity of the bed are sufficiently great and large hydraulic gradients are also present to drive high fluid velocities such as might be the case in high energy losing stream systems [26]. For example, a gravel streambed with an average grainsize of 1 mm and a pore water velocity of 10 m/d would have a Re of around 0.1 ($Pe_{avg} = 0.074$ when $k_s = 2.5 \text{ W(mC)}^{-1}$). However, many streambed environments have smaller grain sizes (silt to sand i.e. 0.01 mm to 1 mm) or smaller pore water velocities due to lower ambient hydraulic gradients such as are often found in lowland settings [7, 14, 27] leading to relatively low Reynolds numbers. For example a sandy streambed ($dp = 0.3 \text{ mm}$) with a pore water velocity of around 0.3 m/d would have a Re of approximately 0.001 ($Pe_{avg} = 7.4 \times 10^{-4}$ when $k_s = 2.5 \text{ W(mC)}^{-1}$).

For $Re < 1$ relevant to many streambed environments, fewer data are available and equation (4) breaks down. Therefore, we propose a correlation based on the only experimental data published to date [28] to calculate the heat transfer coefficient at low Reynolds numbers (down to $Re = 0.001$). These data have been widely used in various studies in the literature [22, 29, 30]. In order to obtain a correlation of the heat transfer in saturated sand, only the part of the Kunii and Smith [28] data related to experimentation with water as the fluid phase and sand and glass beads (with thermal conductivity of 0.5 W(mC)^{-1}) as the solid phase were plotted and analysed (**Figure 1**). The mathematical equation explaining the physics of heat transfer of a single sphere submerged in a fluid is used as the basis of the analysis [31]:

$$Nu = 2.0 + K_1 Pr^p Re^q \quad (7)$$

where, K_1 , p and q are experimental coefficients. It is discussed in Nelson and Galloway [22] that the coefficient of 2 in equation (7) is only valid for single sphere and this coefficient needs to be measured experimentally for real materials. It is also shown by Lienhard [32] that the ratio of thickness of the thermal boundary layer δ_t to that of the fluid boundary layer δ_f equals to:

146 $\frac{\delta_t}{\delta_f} = \text{Pr}^{-\frac{1}{3}}$ for a wide range of gas and fluids $0.6 \leq \text{Pr} \leq 50$. Thus, in derivation of the heat
147 transfer equation the Prandtl number takes the power of 1/3. Therefore, we would expect
148 equation (7) to take the following form:

$$149 \quad Nu = \alpha + K_1 \text{Pr}^{\frac{1}{3}} \text{Re}^q \quad (8)$$

150 We used the software *Datafit* to fit equation (8) to the Kunii and Smith [28] experimental data
151 by varying the parameters α , K_1 and q by a least squares method. The coefficients were
152 chosen from the best fit (details of fitting parameters and confidence intervals can be found in
153 Table A and B in Appendix A). In addition, the model proposed by Nelson and Galloway [22] is
154 also considered to compare the results of each model at $Re=0.01$. The Nelson and Galloway
155 model has been widely used in the industry applications having Reynolds numbers down to 0.01
156 [33, 34]. The model has the form:

$$157 \quad Nu = \frac{2\zeta + \left(\frac{2\zeta^2(1-\phi)^{1/3}}{[1-(1-\phi)^{1/3}]^2} - 2 \right) \tanh \zeta}{\frac{\zeta}{1-(1-\phi)^{1/3}} - \tanh \zeta} \quad (9)$$

$$158 \quad \text{where, } \zeta = 0.3 \left[\frac{1}{(1-\phi)^{1/3}} - 1 \right] \text{Re}^{1/2} \text{Pr}^{1/3}.$$

159 Presented in Figure 1 are also the curves of Nusselt number versus Reynolds numbers for
160 different porosities based on the model of Nelson and Galloway [22]. It is worth noting that the
161 system of one sphere grain in a fluid is assumed to have the porosity of 1. The Nelson and
162 Galloway curves of Figure 1 therefore represent natural sediments at lower to intermediate
163 porosities and at a porosity of 1 the extreme case of heat transfer between fluid and a single
164 sphere.

166 2.2 Forward two-domain numerical model

167 Both the proposed correlation based on the Kunii and Smith [28] data and Nelson and Galloway
168 [22] theory were embedded into a finite element numerical code to forward model the two-
169 temperature equations (1 & 2) for physical parameters typical of streambed materials [11] (also
170 shown in Table 1). In the analysis, Pe was varied by changing the pore water velocity (~ 0.01 ,

0.04, 0.09 and 0.3 m/d) and solid thermal conductivity (the upper and lower bound of thermal conductivity of solids are $k_{s_min} = 0.8 \text{ W(mC)}^{-1}$ and $k_{s_max} = 2.5 \text{ W(mC)}^{-1}$) [35]. While we recognise that this velocity range is at the lower end for typical streambeds, using realistic thermal properties it is as high a range as is possible while staying within the Re range of the Kunii and Smith [28] data on which our heat transfer correlation is based.

For a particular combination of parameters, equations 8 & 9 were solved for Nu and then h_{sf} was extracted from equation 5 and used in equations 1 & 2. In order to solve Eqs. 1 and 2 simultaneously, the initial fluid temperature was used to calculate the solid temperature with the obtained heat transfer coefficient. The obtained solid temperature is then used to calculate new fluid temperature. The i^{th} -step fluid temperature was then compared with $i-1^{\text{th}}$ step fluid temperature using a least square technique to check the convergence. The convergence is considered satisfied for a temperature error of 0.01 °C. A two dimensional mesh with 21 nodes along x-axis (0.1 m) and 8421 nodes along y axis (4.0 m) with 10 mins time steps were used in the numerical simulation. The depth of 4 m to the lower boundary was sufficient to not influence the results extracted from the upper 0.45 m used for the analysis.

Standard Galerkin and Characteristic Galerkin Finite Element discretization techniques [36, 37] with a least square method were used to simultaneously solve for solid and fluid temperatures (equations 1 & 2). Natural heat convection due to buoyancy effects was neglected assuming that the forced convection dominates the heat transfer process [17]. It is also noteworthy that, for the range of Re investigated in this study, the thermal dispersion was negligible [19].

Since most studies of groundwater-surface water interactions using heat as a tracer focus on diel temperature signals, we used a daily sinusoidal upper temperature boundary condition for all model scenarios on top and a constant temperature boundary condition (25°C) at the bottom and no flow boundaries at the sides. The initial temperature across the whole model domain was 25°C. An amplitude of 4°C for the top boundary starting at 25°C (i.e. $T_0 = T_{ave}$) was used for all runs except for one case where sensitivity to the amplitude was tested. A steady state downward fluid flow was assumed and basic physical parameters typical of streambed materials [11] were used. Fluid velocity was varied across a range typically found in the streambed environment for $0.001 < Re < 0.01$. However the heat transfer coefficient used for the analysis was not extrapolated lower than the lower end of Re numbers from the Kunii and Smith [28] experimental data. This

prevents from extracting a superficial magnitude for heat transfer coefficient at very low Reynolds numbers ($Re < 0.001$). Models were run for 100 days and the output from the last day of each run was analysed. The finite element numerical discretization of the governing equations (1 & 2) is presented in Appendix B.

2.3 Inverse single-domain analytical model

The output from the two-domain forward models was used as ‘synthetic field data’ and the amplitude ratios (AR) and phase shifts (PS) of the temperature signal with depth were calculated relative to the upper temperature boundary condition. In a theoretical sense, the fluid and solid temperatures define the upper and lower range of temperature that probes might monitor in streambeds depending on the relative size of the temperature monitoring device and the grain size of the streambed material. In reality, temperature probes will integrate temperature responses from the fluid and solid. However for this analysis, rather than choosing an arbitrary averaging of temperatures which would be site-dependent varying with the type of field instrument used and streambed material, we inverted the data for the fluid and solid separately to show the maximum differences that could arise. Therefore, to represent this range within the synthetic data derived from the forward models, AR s and PS s were calculated for the individual temperatures of the fluid (T_f) and solid (T_s) phases throughout the analysis. The AR and PS values were then inverted using the commonly used equation which assumes LTE [6] via the equations proposed by Hatch et al. [8] (and the ‘known’ porosity and thermal parameters in the forward model) to produce values of pore water velocity at depths of 0.1, 0.2, 0.3, 0.35, 0.4 and 0.45 m. Errors in fluid velocity were calculated by comparing the inverse model results with those used in the forward models. For the inversions the bulk thermal diffusivity, D , was assumed to be given by the following average of the solid and fluid phases:

$$D_{avg} = \frac{(1-\phi)k_s + \phi k_f}{(1-\phi)(\rho c_p)_s + \phi(\rho c_p)_f}$$

In this bulk averaging, the fluid and solid phases are considered as parallel resistors allowing the calculation of the overall energy flux through the system.

3. Results and Discussion

3.1 Heat transfer coefficients for low Reynolds numbers

The best fit correlation of equation (8) to the Kunii and Smith [28] data takes the form:

$$Nu = 2.4 \times 10^{-5} + 285.6 Pr^{\frac{1}{3}} Re^{2.7} \quad (10)$$

The correlation is shown against the data in Figure 1 alongside output from the Nelson-Galloway Model (NGM). For the modelled porosity of 0.3 used here, the agreement between the Kunii and Smith Correlation (KSC) and the NGM is good for practical applications at $Re=0.01$ where the ranges of applicability overlap. This gives confidence in the approach taken here for estimating the heat transfer coefficient. Note that the curves shown for the highest porosities are unrealistic for natural materials but can be realistic for heat transfer within loosely packed beds used in chemical reactors. One sphere grain is assumed to have a porosity of 1 and therefore the curves with higher porosity approach the case of heat transfer between fluid and a single sphere.

3.2 Simulated local thermal non-equilibrium between solid and fluid phases for sinusoidal varying temperature input

Marked differences, up to approximately 1 °C in the modelled cases, were found between the solid and fluid phase temperatures derived from the two-domain model at a range of depths and Pe (and Re) with a surface temperature amplitude of 4 °C and solid thermal conductivity of either 0.8 or 2.5 W(mC)⁻¹. **Figure 2** illustrates this for a depth of 0.2 m and for high and low Re (2.5×10^{-4} and 7.5×10^{-3}). The figure also includes the case with thermal equilibrium (e.g. the Hatch equation [8]) and the purely conductive case for comparison. At the low Re of 2.5×10^{-4} the purely conductive case and the LTE case are producing almost identical temperature fluctuations at 0.2 m depth. This illustrates that for this low Re identifying a velocity different from zero probably leads to inaccuracy. However, for the two-domain model the temperature fluctuations for solid and fluid differ from each other as well as from the conductive and the LTE cases (both in terms of amplitude and phase). It is interesting to note that the temperature fluctuations for the solid and fluid cannot be combined (by some weighed average) to produce the one-domain analytical LTE temperature fluctuations since they are both simultaneously lower (or both higher) than the LTE temperature. At higher Re ($=7.5 \times 10^{-3}$), there is now a distinct difference between the conductive case and the LTE case. However, the temperature of fluid and solid from the two-domain model and LTE case are almost identical for high and low

solid thermal conductivities showing that the two-domain system is approaching thermal equilibrium.

We extracted the difference between the sinusoid amplitude of the solid and fluid temperatures (ATD) as a measure of the thermal disequilibrium. In order to investigate the effect of change in amplitude of surface temperature on ATD at different Reynolds numbers, four temperature sinusoids with amplitude of 1, 2, 3 and 4°C were applied on the surface boundary (**Figure 3**) and the response was measured at 0.2 m depth. In this analysis, the volumetric heat transfer coefficient ($h_{sf}a_{sf}$ in equation 2) was set constant ($200 \text{ W(m}^3\text{C)}^{-1}$, $Re = 0.0056$) in order to analyse only the effect of velocity on ATD (and neglect the effect of heat transfer coefficient). **Figure 3** indicates that the lower the temperature amplitude applied at the top boundary the lower the resultant ATD. Moreover, the increase in velocity gives rise to increasing values for ATD particularly when it passes the threshold of $Pe = 0.0074$ (or $Re=0.01$). This is due to the fact that an increase in velocity leads to a higher localised temperature gradient at the grain boundary; greater thermal non-equilibrium occurs in these modelled conditions as conduction into the grains cannot keep pace with the advective flux of heat through the fluid (i.e. higher grain Pe).

3.3 Error in derived streambed fluid velocity when assuming local thermal equilibrium

The relative ($\frac{v_{ARorPS} - v_{actual}}{v_{actual}}$) and absolute ($v_{ARorPS} - v_{actual}$) errors in pore water velocity (from both the AR and PS [8]) using T_s , or T_f as a function of Pe are presented in **Figure 4a-d**. From **Fig. 4**, the errors in derived velocity estimates converge to zero value for all cases as Pe increases whether using T_s , or T_f except the PS velocity errors obtained from T_f and high solid thermal conductivity (k_{high}). So, while the increase in advective flux (Pe) tends to thermally disequilibrate the system (**Fig. 3**), this is more than compensated by an increased heat transfer coefficient (h_{sf}) at higher velocities which tends to increase equilibrium between phases, leading to more equilibrium at higher Pe (Re) in the range considered here (This is summarised conceptually in **Fig. 7**).

It can be seen from **Fig. 4** that the AR derived relative and absolute velocity errors are negative and decrease with depth using T_f and high solid thermal conductivity (k_{high}) at low Pe (low Re), whereas the errors are positive using T_s with the same k_{high} and at low Pe . This is attributed to

the fact that AR values of the solid and fluid phases are different to that of the local thermal equilibrium case (i.e. AR derived from the 1-D analytical solution based on the LTE assumption). In order to compare the AR values of the numerical analysis to that of the analytical solution at different Re ($=2.5 \times 10^{-4}$ and 7.5×10^{-4}) **Fig. 5** is presented (it should be noted that Pe is replaced with Re in Fig. 5 due to the fact that Pe varies with change in solid thermal conductivity).

As an example, the AR values of the solid phase, with high solid thermal conductivity (k_{high}) at low Pe ($Re=2.5 \times 10^{-4}$), are higher than that of the local thermal equilibrium case leading to higher derived velocities than for the LTE case and thus positive errors. AR values of the fluid phase, with high solid thermal conductivity (k_{high}) at low Pe ($Re=2.5 \times 10^{-4}$), are lower leading to lower velocities than the LTE case and thus negative errors. It can also be seen from Fig. 2 that the temperature fluctuations of the LTE case is lower than the temperature fluctuations of the solid phase with k_{high} and higher than the temperature fluctuations of the fluid at low Pe ($Re=2.5 \times 10^{-4}$). The physical basis for these deviations is that at low Pe , the heat exchange between phases becomes inefficient and therefore, using k_{high} , the heat transport in the solid phase becomes much quicker than that within the fluid.

Using a lower solid thermal conductivity (k_{low}) and low Pe ($Re=2.5 \times 10^{-4}$), on the other hand, the AR s using either T_s or T_f are both greater than those for the local thermal equilibrium case and therefore positive velocity errors are obtained. Again it can be explained by the fact that at low Pe the heat exchange between phases is inefficient and since the solid thermal conductivity is low (very close to fluid thermal conductivity) the solid and fluid phases end up behaving similarly. The reason why the AR value of the LTE case is slightly lower than both the solid and fluid AR s is because of the difference in the thermal diffusivity of each phase and that of the LTE case. Although the thermal conductivity of the LTE case sits between the solid and fluid thermal conductivities, its thermal diffusivity may sit between or below the solid and thermal phases due to a different volumetric heat capacity. And because the thermal diffusivity affects the rate of heat transfer, lower magnitude of AR is observed compared to that of solid and fluid (where the thermal diffusivity of LTE case sits below the solid and thermal phases). It is noteworthy that the diffusivity is the function of both the thermal conductivity and the

volumetric heat capacity. When moving toward higher Pe ($Re=7.5\times 10^{-4}$), the error approaches zero showing that the system reaches local thermal equilibrium.

The relative errors in the PS derived velocity estimates (Fig. 4) have similar trends and greater magnitudes compared to those derived using AR s especially at lower end of Pe . From Fig. 4d, it can be seen that the PS derived absolute velocity errors stay constant at relatively lower velocities (Pe). Thus the relative errors increase only due to a reduction in the actual pore water velocity. Due to the fact that the AR and PS methods are sensitive to different velocities [8], the PS method loses its sensitivity at lower range of velocity and the same velocity estimate is returned. In addition, the errors at higher velocities do not converge to the absolute zero which is resulted from the effect of local thermal non-equilibrium on the phase shift of the temperature data. The obtained PS values of the numerical analysis and analytical solution at different Re ($=2.5\times 10^{-4}$ and 7.5×10^{-4}) are also presented in **Fig. 6** for comparison.

Since the errors we have reported here are significant, especially for relatively low Pe (relative errors up to 30 and 150 are obtained from AR and PS), we have compared the parameter range of our results to laboratory studies which present data with which it is possible to assess the robustness of a single-domain equation (implicitly assuming the validity of LTE) in deriving stream bed velocities using diurnal temperature signals. Surprisingly, given the ever increasing number of field applications using such an approach there are, to our knowledge, only 3 laboratory studies of relevance. Rau et al. [19] found generally good agreement between experimental and theoretical expectations in a study conducted at a range of Re above the data presented here, in the range where we would expect the LTE assumption to be valid. Munz et al. [38] and Lautz [39] present results which may cross over with the range of Re we have analysed here although, unfortunately, neither paper is explicit regarding the grain size distribution used in their experiments. However, using a typical range of grain sizes for fine sand [39] and medium sand [38] the minimum Re studied may have been approximately $6\cdot 10^{-3}$ and $2.5\cdot 10^{-3}$ respectively which are within the range of values where we would expect LTE to breakdown. In the Lautz [39] experiments, we note that significant discrepancies were found between velocities derived using AR and PS , which remain unexplained and that might be due to LTNE, although other effects such as heterogeneity can also induce such discrepancies [40, 41].

In the Munz et al. [38] experiments, increasing discrepancies are apparent between the measured and modelled flow velocities as the flow rate decreases. These observations are consistent with the understanding of LTNE described in this paper, and we propose that false assumptions of LTE may have contributed to these reported errors.

The errors that could arise due to a false assumption of LTE may be of the same order of magnitude as errors due to other factors such as non-uniform flow fields [10, 11], sediment heterogeneity [12], measurement error and difficulties in estimating thermal parameters [13, 14].

4. Conclusion

Despite a large body of literature describing the fundamentals of heat transfer in porous media, the plethora of studies which have applied heat as a tracer in streambeds have, to our knowledge without exception, assumed local thermal equilibrium between solid and fluid phases. However, there is evidence from existing theory and empirical evidence that this assumption may not be valid in many instances [22, 28].

Here we have derived a correlation for the heat transfer coefficient at low Re using well known experimental data (KSC) which is in good agreement with a physically based model (NGM). Our analysis reveals that two main mechanisms control the degree of thermal equilibrium between the solid and fluid phases in a typical streambed: the ratio of the conductive to advective heat transport (described by the grain thermal Pe) and the heat transfer coefficient which is related to the Re (Figure 7). These processes act against each other; higher advection tends towards disequilibrium between phases while at high velocities this process is more than outweighed by an increasing heat transfer coefficient which tends to move the system towards equilibrium. Including these processes in a two-domain heat transport model we have shown that the LTE assumption may break down at $Re < 0.01$ for typical streambed thermal parameters. Furthermore, this model output was then inverted using a 1D analytical model which assumes LTE, to show that considerable relative errors in streambed velocity estimates may result at low Re (or Pe) if the possibility of LTNE is ignored. In general, these errors are higher at relatively lower Re and may lead to significant inferred flows from data inversions based on the LTE assumption (0.3 m/d using AR and 1.3 m/d using PS) when in fact the real flow is small or zero. Such errors may be of the same order of magnitude as other known uncertainties in streambed heat tracing [10-14].

These results have important implications for interpreting and predicting streambed temperature dynamics, critical for improving the understanding of controls on stream ecology and biogeochemical processes. More laboratory studies are urgently needed to supplement the sparse existing data in this area and further test the findings of this study. In particular, the data and models on which this study is based was for homogeneous media and diel temperature signals, and it is to be expected that results will significantly differ for real field conditions; such data are required to enable a more complete physical understanding of heat transport processes in real streambeds to be derived.

Acknowledgments

Funding for this research was provided by the National Centre for Groundwater Research and Training, an Australian Government initiative, supported by the Australian Research Council and the National Water Commission. Mark Cuthbert acknowledges funding by the European Community's Seventh Framework Programme [FP7/2007-2013] under grant agreement n°299091.

Appendix A

Table A. Details of fitting parameters to the experimental data of Kunii and Smith [1961] in Figure 1 using DATAFIT software.

Results from project "LTNE"	
Model Definition:	$Nu/Pr^2 = a + b \cdot Re^c$ Where $a = \alpha/Pr^2$, $b = K_1 \times Pr^{(1/3)}/Pr^2$ and $c = q$
Number of observations	41
Number of missing observations	0
Solver type	Nonlinear
Nonlinear iteration limit	250
Diverging nonlinear iteration limit	10
Number of nonlinear iterations performed	61
Residual tolerance	1.00E-10
Sum of Residuals	9.31E-15
Average Residual	2.27E-16
Residual Sum of Squares (Absolute)	3.63E-11
Residual Sum of Squares (Relative)	3.63E-11
Standard Error of the Estimate	9.78E-07
Coefficient of Multiple Determination (R^2)	8.37E-01
Proportion of Variance Explained	83.68%
Adjusted coefficient of multiple determination (R_a^2)	0.83
Durbin-Watson statistic	1.53

Table B. Regression variable results for the experimental data of Kunii and Smith [1961] including the best fit and confidence intervals of 68%, 90%, 95% and 99% from DATAFIT software.

Variable	Value	Standard	t-ratio	Prob(t)
A	7.35E-07	4.48E-07	1.640975375	0.10906
B	15.3962065	42.61194092	0.361312021	0.71987
C	2.687445266	0.51686944	5.199466357	0.00001
68% Confidence				
Variable	Value	68% (+/-)	Lower	Upper
A	7.35E-07	4.51E-07	2.84E-07	1.19E-06
B	15.3962065	42.93579167	-	58.33199817
C	2.687445266	0.520797648	2.166647618	3.208242914
90% Confidence				
Variable	Value	90% (+/-)	Lower	Upper
A	7.35E-07	7.55E-07	-2.02E-08	1.49E-06
B	15.3962065	71.84373239	-	87.23993889
C	2.687445266	0.871441876	1.816003389	3.558887142
95% Confidence				
Variable	Value	95% (+/-)	Lower	Upper
A	7.35E-07	9.07E-07	-1.72E-07	1.64E-06
B	15.3962065	86.2636132	-70.8674067	101.6598197
C	2.687445266	1.046350495	1.641094771	3.73379576
99% Confidence				
Variable	Value	99% (+/-)	Lower	Upper
A	7.35E-07	1.21E-06	-4.80E-07	1.95E-06
B	15.3962065	115.5422778	-	130.9384843
C	2.687445266	1.401491487	1.285953778	4.088936753
Variance Analysis				
Source	DF	Sum of	Mean	F Ratio
Regression	2	1.86E-10	9.32E-11	97.42871476
Error	38	3.63E-11	9.56E-13	
Total	40	2.23E-10		

Appendix B

Numerical discretization: the standard and Characteristic Galerkin techniques are used to discretize the governing equations of the two-domain heat transport problem (equations 1 and 2). It results in the following system of equations for a two dimensional problem:

$$[-(M + \Delta t[H - M_3])][\Delta \vec{T}_i^s] = [\Delta t[H - M_3]T_i^s(t_{i-1}) - \Delta t M_3 T_i^f(t_i)]$$

$$[-(M + \Delta t(C - K_1 - K_2) - \Delta t M_2)][\Delta \vec{T}_i^f] = [\Delta t[(C - K_1 - K_2) - M_2]T_i^f(t_{i-1}) + \Delta t M_2 T_i^s(t_i)]$$

where i is the time step; \vec{T} is the temperature vector; $\vec{T}_T = (T_1 \ T_2 \ \dots \ T_n)$; T is the nodal temperature; subscripts s and f represent the solid and fluid phases respectively; Δt represents the time increment and the matrices are defined as:

$$\vec{M} = \int_{V_e} [N_T]^T [N_T] dV$$

$$\vec{C} = \int_{V_e} [N_T]^T \frac{\partial}{\partial x} \left(\frac{1}{\phi} \left(\frac{\langle k \rangle^f}{(\rho c_p)_f} + f(\vec{\beta}, \vec{v}_x) \right) \frac{\partial [N_T]}{\partial x} \right) \{\chi\}^n dV + \int_{V_e} [N_T]^T \frac{\partial}{\partial y} \left(\frac{1}{\phi} \left(\frac{\langle k \rangle^f}{(\rho c_p)_f} + f(\vec{\beta}, \vec{v}_y) \right) \frac{\partial [N_T]}{\partial y} \right) \{\chi\}^n dV$$

$$\vec{K}_1 = v_x^d \int_{V_e} [N_T]^T \frac{\partial [N_T]}{\partial x} \{\chi\}^n dV + v_y^d \int_{V_e} [N_T]^T \frac{\partial [N_T]}{\partial y} \{\chi\}^n dV$$

$$\vec{K}_2 = \frac{\Delta t}{2} v_x^d \int_{V_e} \left[\frac{\partial}{\partial x} (v_x^d \frac{\partial [N_T]}{\partial x} \{\chi\}^n + v_y^d \frac{\partial [N_T]}{\partial y} \{\chi\}^n) \right] dV + \frac{\Delta t}{2} v_y^d \int_{V_e} \left[\frac{\partial}{\partial y} (v_x^d \frac{\partial [N_T]}{\partial x} \{\chi\}^n + v_y^d \frac{\partial [N_T]}{\partial y} \{\chi\}^n) \right] dV$$

$$\vec{M}_2 = \int_{V_e} \frac{h_{sf} a_{sf}}{\phi (\rho c_p)_f} [N_T]^T [N_T] dV$$

$$\vec{M}_3 = \int_{V_e} \frac{h_{sf} a_{sf}}{(1-\phi)(\rho c_p)_s} [N_T]^T [N_T] dV$$

$$\vec{H} = \int_{V_e} [N_T]^T \frac{\partial}{\partial x} \left(\frac{\langle k \rangle^s}{(1-\phi)(\rho c_p)_s} \frac{\partial [N_T]}{\partial x} \right) \{\chi\}^n dV + \int_{V_e} [N_T]^T \frac{\partial}{\partial y} \left(\frac{\langle k \rangle^s}{(1-\phi)(\rho c_p)_s} \frac{\partial [N_T]}{\partial y} \right) \{\chi\}^n dV$$

where N_T is the finite element shape function of temperature, V is the spatial area of an element and χ is the variable.

References

- [1] Krause S, DM Hannah, JH Fleckenstein, CM Heppell, D Kaeser, R Pickup, et al. Interdisciplinary perspectives on processes in the hyporheic zone. *Ecohydrology*. 4 (2011) 481-99, doi: 10.1002/eco.176.
- [2] Kaplan LA, TL Bott. Diel fluctuations in bacterial activity on streambed substrata during vernal algal blooms: Effects of temperature, water chemistry, and habitat. *Limnol Oceanogr*. 34 (1989) 118-733.
- [3] Evans EC, GE Petts. Hyporheic temperature patterns within riffles. *Hydrological Sciences Journal*. 42 (1997) 199-213, doi: 10.1080/02626669709492020.
- [4] Brunke M, TOM Gonser. The ecological significance of exchange processes between rivers and groundwater. *Freshwater Biology*. 37 (1997) 1-33, doi: 10.1046/j.1365-2427.1997.00143.x.
- [5] Constantz J. Heat as a tracer to determine streambed water exchanges. *Water Resources Research*. 44 (2008) W00D10, doi: 10.1029/2008WR006996.
- [6] Stallman RW. Steady One-Dimensional Fluid Flow in a Semi-Infinite Porous Medium with Sinusoidal Surface Temperature. *J Geophys Res*. 70 (1965) 2821-7, doi: 10.1029/JZ070i012p02821.
- [7] Keery J, A Binley, N Crook, JWN Smith. Temporal and spatial variability of groundwater-surface water fluxes: Development and application of an analytical method using temperature time series. *Journal of Hydrology*. 336 (2007) 1-16, doi: 10.1016/j.jhydrol.2006.12.003.
- [8] Hatch CE, AT Fisher, JS Revenaugh, J Constantz, C Ruehl. Quantifying surface water-groundwater interactions using time series analysis of streambed thermal records: Method development. *Water Resour Res*. 42 (2006) W10410, doi: 10.1029/2005wr004787.
- [9] Wörman A, J Riml, N Schmadel, BT Neilson, A Bottacin-Busolin, JE Heavilin. Spectral scaling of heat fluxes in streambed sediments. *Geophysical Research Letters*. 39 (2012) L23402, doi: 10.1029/2012GL053922.
- [10] Cuthbert MO, R Mackay. Impacts of nonuniform flow on estimates of vertical streambed flux. *Water Resources Research*. 49 (2013) 19-28, doi: 10.1029/2011WR011587.
- [11] Roshan H, GC Rau, MS Andersen, IR Acworth. Use of heat as tracer to quantify vertical streambed flow in a two-dimensional flow field. *Water Resources Research*. 48 (2012) W10508, doi: 10.1029/2012WR011918.
- [12] Ferguson G, V Bense. Uncertainty in 1D Heat-Flow Analysis to Estimate Groundwater Discharge to a Stream. *Ground Water*. 49 (2011) 336-47, doi: 10.1111/j.1745-6584.2010.00735.x.
- [13] Shanafield M, C Hatch, G Pohll. Uncertainty in thermal time series analysis estimates of streambed water flux. *Water Resour Res*. 47 (2011) W03504, doi: 10.1029/2010wr009574.
- [14] Cuthbert MO, R Mackay, V Durand, MF Aller, RB Greswell, MO Rivett. Impacts of river bed gas on the hydraulic and thermal dynamics of the hyporheic zone. *Advances in Water Resources*. 33 (2010) 1347-58, doi: <http://dx.doi.org/10.1016/j.advwatres.2010.09.014>.
- [15] Nield DA, A Bejan. *Convection in Porous Media*. Third Edition ed. SPRINGER, 2006.
- [16] Kaviani M. *Principles of Heat Transfer in Porous Media*. 2nd ed. Springer, 1995.
- [17] Amiri A, K Vafai. Analysis of dispersion effects and non-thermal equilibrium, non-Darcian, variable porosity incompressible flow through porous media. *International Journal of Heat and Mass Transfer*. 37 (1994) 939-54, doi: 10.1016/0017-9310(94)90219-4.
- [18] Alazmi B, K Vafai. Analysis of Variable Porosity, Thermal Dispersion, and Local Thermal Nonequilibrium on Free Surface Flows Through Porous Media. *Journal of Heat Transfer*. 126 (2004) 389-99.

- [19] Rau GC, MS Andersen, RI Acworth. Experimental investigation of the thermal dispersivity term and its significance in the heat transport equation for flow in sediments. *Water Resour Res.* 48 (2012) W03511, doi: 10.1029/2011wr011038.
- [20] Vafai K, M Sozen. Analysis of Energy and Momentum Transport for Fluid Flow Through a Porous Bed. *Journal of Heat Transfer.* 112 (1990) 690-9.
- [21] Wakao N, S Kaguei, T Funazkri. Effect of fluid dispersion coefficients on particle-to-fluid mass transfer coefficients in packed beds: Correlation of sherwood numbers. *Chemical Engineering Science.* 33 (1978) 1375-84, doi: 10.1016/0009-2509(78)85120-3.
- [22] Nelson PA, TR Galloway. Particle-to-fluid heat and mass transfer in dense systems of fine particles. *Chemical Engineering Science.* 30 (1975) 1-6, doi: 10.1016/0009-2509(75)85109-8.
- [23] Verschoor H, GCA Schuit. Heat transfer to fluids flowing through a bed of granular solids. *Appl sci Res.* 2 (1951) 97-119, doi: 10.1007/BF00411975.
- [24] Gupta AS, G Thodos. Transitional Behavior for the Simultaneous Mass and Heat Transfer of Gases Flowing through Packed and Distended Beds of Spheres. *Industrial & Engineering Chemistry Fundamentals.* 3 (1964) 218-20, doi: 10.1021/i160011a008.
- [25] McConnachie JTL, G Thodos. Transfer processes in the flow of gases through packed and distended beds of spheres. *AIChE Journal.* 9 (1963) 60-4, doi: 10.1002/aic.690090113.
- [26] Wang W, J Li, W Wang, X Chen, D Cheng, J Jia. Estimating streambed parameters for a disconnected river. *Hydrological Processes.* (2013) accepted May 2013, doi: 10.1002/hyp.9904.
- [27] Jensen JK, P Engesgaard. Nonuniform Groundwater Discharge across a Streambed: Heat as a Tracer. *Vadose Zone Journal.* 10 (2011) 98-109, doi: 10.2136/vzj2010.0005.
- [28] Kunii D, JM Smith. Heat transfer characteristics of porous rocks: II. Thermal conductivities of unconsolidated particles with flowing fluids. *AIChE Journal.* 7 (1961) 29-34, doi: 10.1002/aic.690070109.
- [29] Jiang P-X, R-N Xu, W Gong. Particle-to-fluid heat transfer coefficients in miniporous media. *Chemical Engineering Science.* 61 (2006) 7213-22, doi: 10.1016/j.ces.2006.08.003.
- [30] Cybulski A, MJ Van Dalen, JW Verkerk, PJ Van Den Berg. Gas-particle heat transfer coefficients in packed beds at low Reynolds numbers. *Chemical Engineering Science.* 30 (1975) 1015-8, doi: 10.1016/0009-2509(75)87002-3.
- [31] Ranz WE. Evaporation from drops: Part I. *Chem Engng Progr.* 48 (1952).
- [32] Lienhard JH. A Heat Transfer TextBook. Third ed. Phlogiston Press, 2008.
- [33] Scala F. Particle-fluid mass transfer in multiparticle systems at low Reynolds numbers. *Chemical Engineering Science.* 91 (2013) 90-101, doi: <http://dx.doi.org/10.1016/j.ces.2013.01.012>.
- [34] Rowe PN. Particle-to-liquid mass transfer in fluidised beds. *Chemical Engineering Science.* 30 (1975) 7-9, doi: [http://dx.doi.org/10.1016/0009-2509\(75\)85110-4](http://dx.doi.org/10.1016/0009-2509(75)85110-4).
- [35] Farouki OT. Thermal properties of soils. U.S. Army Cold Regions Research and Engineering Laboratory 1981.
- [36] Zienkiewicz O, R Taylor. The finite element method, basic formulation and linear problems. Butterworth-Heinemann, Oxford, 2000.
- [37] Lewis RW, P Nithiarasu, KN Seetharamu. Fundamentals of the Finite Element Method for Heat and Fluid Flow. John Wiley 2004.
- [38] Munz M, SE Oswald, C Schmidt. Sand box experiments to evaluate the influence of subsurface temperature probe design on temperature based water flux calculation. *Hydrology and Earth System Sciences.* 15 (2011) 3495-510.

- [39] Lautz LK. Observing temporal patterns of vertical flux through streambed sediments using time-series analysis of temperature records. *Journal of Hydrology*. 464–465 (2012) 199–215, doi: <http://dx.doi.org/10.1016/j.jhydrol.2012.07.006>.
- [40] Luce CH, D Tonina, F Gariglio, R Applebee. Solutions for the diurnally forced advection-diffusion equation to estimate bulk fluid velocity and diffusivity in streambeds from temperature time series. *Water Resources Research*. 49 (2013) 488–506, doi: 10.1029/2012WR012380.
- [41] McCallum AM, MS Andersen, GC Rau, RI Acworth. A 1-D analytical method for estimating surface water–groundwater interactions and effective thermal diffusivity using temperature time series. *Water Resources Research*. 48 (2012) W11532, doi: 10.1029/2012WR012007.

Figure 1 Variation of Nu with Re : Kunii & Smith (1961) experimental data alongside our correlation and the Nelson Galloway Model (NGM) results for a variety of porous material porosities (ϕ).

Figure 2 Sinusoidal temperature fluctuations at the surface and at 0.2 m depth for Re numbers of 7.5×10^{-3} and 2.5×10^{-4} and high (2.4 W(mC)^{-1}) and low (0.8 W(mC)^{-1}) solid thermal conductivities. Temperatures were calculated for the solid and the fluid by the two-domain model (as outlined in the methodology), and for the assumption of local thermal equilibrium (LTE) using the method by Hatch et al. [8] and for the case of no flow (thermal diffusion only).

Figure 3. the amplitude of the temperature difference (ATD) as a function of Re at four different temperature amplitudes (1, 2, 3 and 4 °C) at the stream-sediment temperature boundary condition. For this simulation the heat transfer coefficient has been held constant and the depth of measurement is 0.2 m.

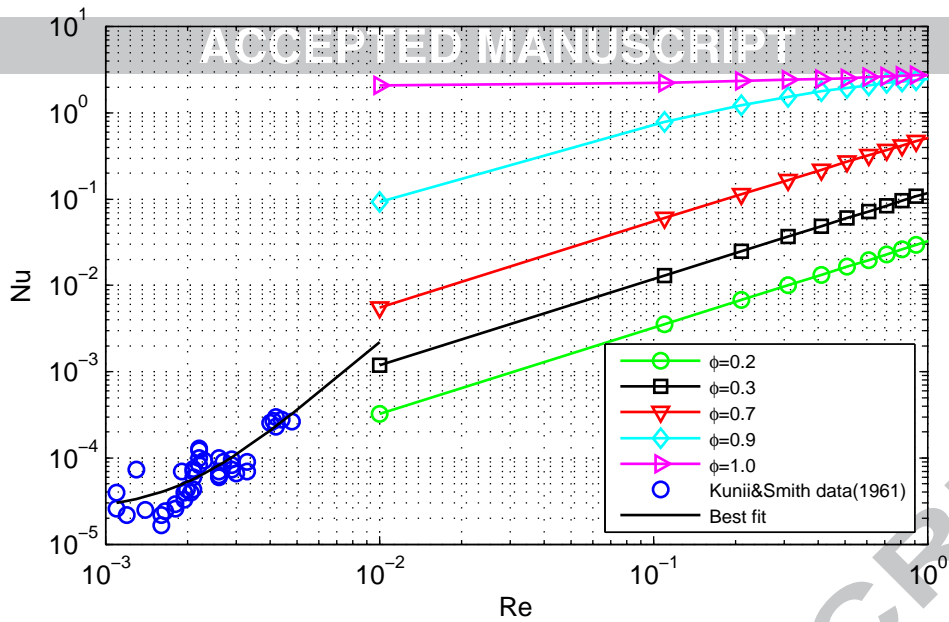
Figure 4. a) AR derived relative velocity error, b) PS derived relative velocity error c) AR derived absolute velocity error and d) PS derived absolute velocity error vs Pe_{avg} using solid and fluid phase temperatures and higher and lower values of solid thermal conductivity ($k_{s_min}=0.8 \text{ W(mC)}^{-1}$ and $k_{s_max}=2.4 \text{ W(mC)}^{-1}$). The velocity range is ~ 0.01 - 0.3 m/d . For all plots the set of curves for each symbol represents velocity error estimates for depths of 0.1, 0.2, 0.3, 0.35, 0.4 and 0.45 m.

Figure 5. The amplitude ratio (AR) of the temperature signal vs depth at high ($=7.5 \times 10^{-3}$) and low ($=2.5 \times 10^{-4}$) Reynolds numbers for high and low solid thermal conductivities using solid and fluid temperatures. Also shown are the AR s derived using the 1-D analytical solution which assumes LTE [Hatch et al, 2006].

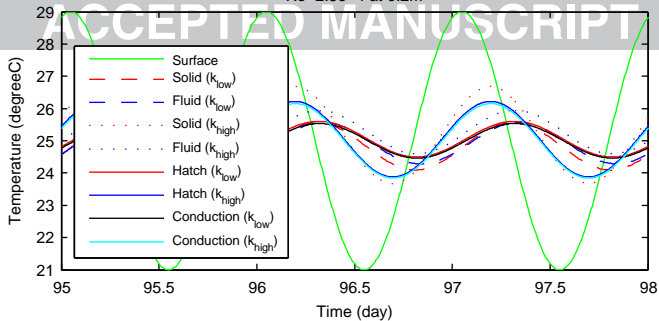
Figure 6. The phase shift (PS) of the temperature signal (PS) vs depth at high ($=7.5 \times 10^{-3}$) and low ($=2.5 \times 10^{-4}$) Reynolds numbers for high and low solid thermal conductivities using solid and fluid temperatures. Also shown are the PS derived using the 1-D analytical solution which assumes LTE [Hatch et al, 2006].

Figure 7. The relative importance of advective heat transport through the fluid, and heat transfer between the solid and the fluid phases at high and low Re . a) At low flow rates the heat transfer is relatively inefficient at thermally equilibrating the solid and fluid phases and LNTE is possible. b) At high rates of fluid advection (high Pe) even though heat is advected fast through the porous media the heat transfer is far more efficient and helps maintain LTE.

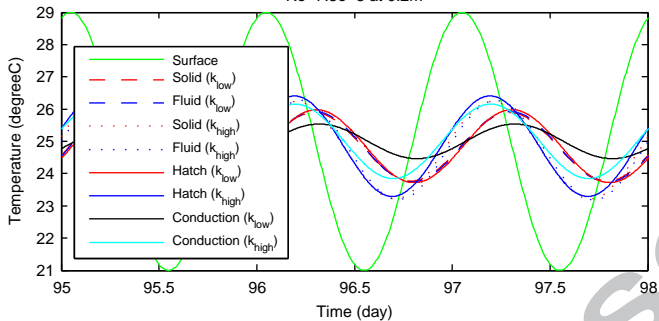
Table 1. Physical data used in the study.

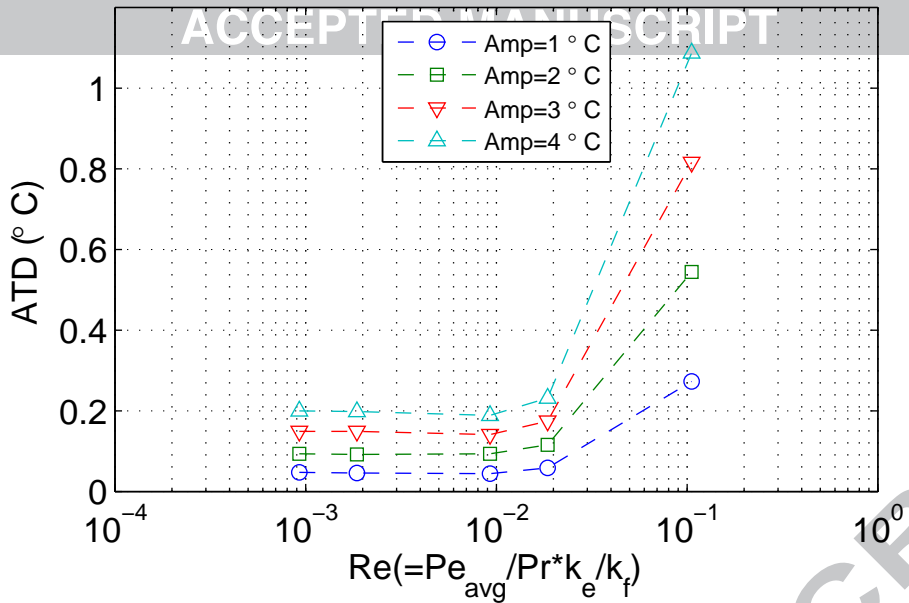


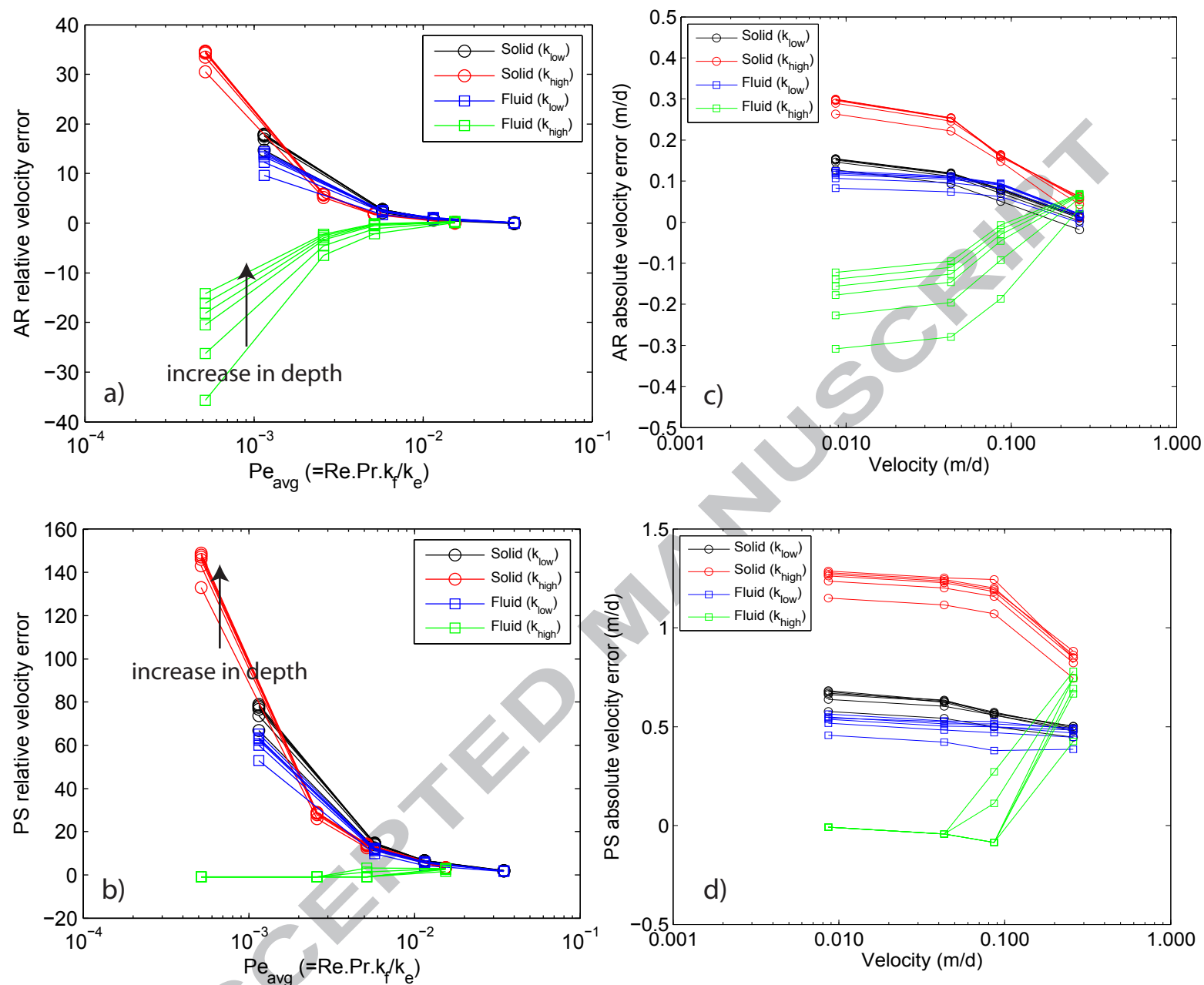
Re=2.5e-4 at 0.2m



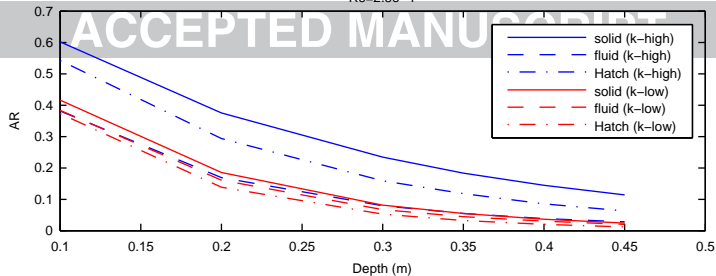
Re=7.5e-3 at 0.2m



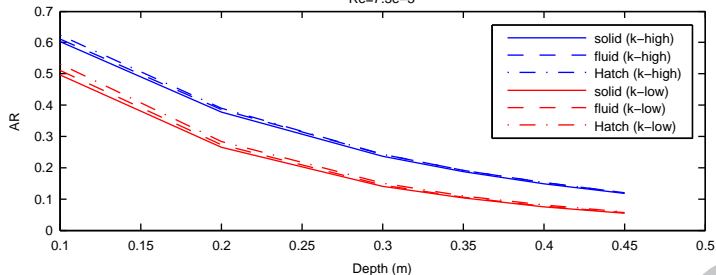


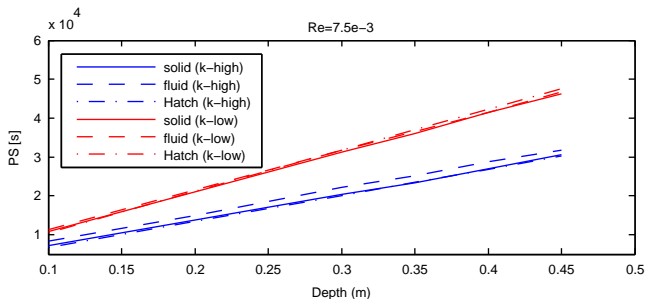
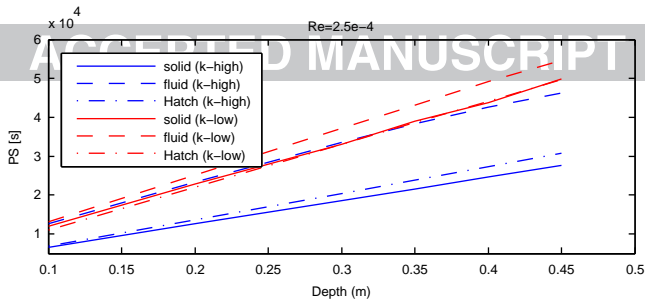


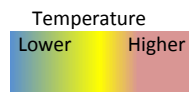
Re=2.5e-4



Re=7.5e-3

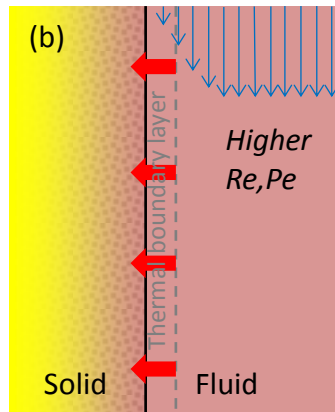
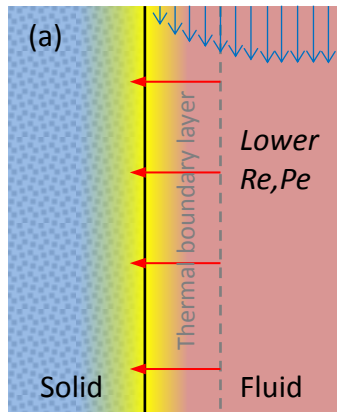






Relative rate
of fluid-solid
heat exchange

Relative rate
of fluid
advection



637 Table 1

Parameter	Unit	Symbol	Value
Solid Thermal Conductivity	$\text{W}(\text{mC})^{-1}$	$k_{s_min} \text{ \& } k_{s_min}$	0.8 \& 2.5
Water Thermal Conductivity	$\text{W}(\text{mC})^{-1}$	k_f	0.58
Water Specific Heat Capacity	$\text{J}(\text{kgC})^{-1}$	c_f	4183
Solid Specific Heat Capacity	$\text{J}(\text{kgC})^{-1}$	c_s	750
Water Density	kg m^{-3}	ρ_f	999.7
Solid Density	kg m^{-3}	ρ_s	2650
Porosity	-	ϕ	0.3
Longitudinal Thermal Dispersivity	s	β_l	1.478
Transverse Thermal Dispersivity	s	β_t	0.4

638

639

Highlights

- We have derived a correlation for heat transfer coefficient at low Re
- Local thermal equilibrium may not be a valid assumption in sediments' heat transfer
- Error in temperature derived velocity estimates may be obtained using LTE